

February 15, 2010

**Molecular hydrogen impacts chalcopyrite bioleaching by the extremely
thermoacidophilic archaeon *Metallosphaera sedula***

Kathryne S. Auernik and Robert M. Kelly*

*Department of Chemical and Biomolecular Engineering
North Carolina State University
Raleigh, NC 27695-7905*

Submitted to: **Applied and Environmental Microbiology** (August, 2009)

AEM02016 Version 3 submitted, February, 2010

Running title: H₂ impact on *Metallosphaera sedula* CuFeS₂ leaching

Keywords: *Metallosphaera sedula*, extreme thermoacidophile, bioleaching,
iron oxidation, hydrogen oxidation

*Address correspondence to: **Robert M. Kelly**
Department of Chemical and Biomolecular Engineering
North Carolina State University
EB-1, 911 Partners Way
Raleigh, NC 27695-7905
Phone: (919) 515-6396
Fax: (919) 515-3465
Email: rmkelly@eos.ncsu.edu

ABSTRACT

Hydrogen served as a competitive inorganic energy source, impacting the CuFeS_2 bioleaching efficiency of the extremely thermoacidophilic archaeon *Metallosphaera sedula*. ORFs encoding key terminal oxidase and electron transport chain components were triggered by CuFeS_2 . Evidence of heterotrophic metabolism was noted after extended periods of bioleaching, presumably related to cell lysis.

For bioleaching processes focused on the recovery of base, precious and strategic metals from low-grade ores, most microorganisms studied to date are mesophilic bacteria (19). However, moderately and extremely thermoacidophilic archaea may be advantageous in certain bioleaching applications and should be considered (7, 8, 12). For chalcopyrite (CuFeS_2) bioleaching, for example, higher temperatures can lead to faster overall leaching kinetics, in part by minimizing passivation, which slows rates at the mineral surface (16, 17). *Metallosphaera sedula*, an extremely thermoacidophilic, metal-mobilizing crenarchaeon growing optimally at 70-75°C and pH 2 (3), has been examined in this regard (7, 11). Key to bioleaching capacity in this microorganism is the dissimilatory oxidation of iron and sulfur, mediated by membrane-associated electron transport chains that are anchored by terminal oxidases (2, 3, 13). For *M. sedula*, another factor that needs to be considered is the impact of inorganic energy sources, other than metal sulfides, has on bioleaching. This issue was considered here by examining the influence of molecular hydrogen on *M. sedula* CuFeS_2 bioleaching.

M. sedula (DSMZ 5348) was grown aerobically at 70°C in an orbital bath (70 rpm). Autotrophic cultures (headspace content: 7% CO_2 , 14% O_2 , 28% H_2 , balance N_2) were used to inoculate 1 L bottles containing 300 mL of DSMZ medium 88 (pH 2), supplemented with 10 g/L chalcopyrite (provided by Greg Olsen, Geosynfuels, Golden, CO), and a headspace of either air, air + CO_2 (7% final concentration), or the autotrophic mix mentioned above. Cells were enumerated using epifluorescence microscopy with acridine orange stain. Cultures growing exponentially were harvested 1 day post-inoculation and compared to CuFeS_2 -grown cultures that were harvested 3 or 9 days post-inoculation. Harvesting was done as previously described (2, 3). Methods used for microarray construction, RNA preparation, slide scanning, and data analysis were also as described previously, with the exception that Trizol (Invitrogen) was used as the RNA extraction reagent and a Packard BioChip Scanarray 4000 scanner was used for slide scanning. Significant differential

transcription, or “response,” was defined as relative changes ≥ 2 (where a log₂ value of ± 1 means a two-fold change) having significance values ≥ 5.4 (Bonferroni correction equivalent to a p-value of 4.0×10^{-6} for this microarray configuration). Soluble iron and its oxidation state in *M. sedula* cultures were tracked using an o-phenanthroline colorimetric assay modified from ASTM E3934 and (15). Transcriptional response data are available through the NCBI Gene Expression Omnibus (GEO) database under accession number (to be provided upon acceptance of manuscript for publication).

Ferric iron precipitation is minimized during bioleaching in the presence of H₂.

Chalcopyrite bioleaching in *M. sedula* cultures was compared to abiotic controls 9 days post-inoculation. Visual inspection of chalcopyrite cultures with an air-only headspace revealed evidence of biotic activity (rust-colored precipitate) when compared to their abiotic control. However, no visual evidence of ferric iron formation was evident for cultures growing in an H₂-containing headspace or their abiotic control (**Figure 1A**). Measurement of soluble iron (almost entirely in the reduced Fe²⁺ state) for H₂-containing conditions showed accumulation of significantly greater amounts of iron in inoculated cultures compared to their abiotic control (**Figure 1B**). This indicated that bioleaching was also occurring in the H₂-supplemented cultures, despite an absence of ferric iron precipitates typically associated with bioleaching activity. It was unclear how the presence of H₂ correlated with the absence of extensive precipitate formation. The absence of significant amounts of ferric iron in solution for all abiotic controls suggests that the rate of reduction/consumption of ferric iron by the Cu-containing bioleaching substrate may be higher than for pyritic substrates without Cu (where significant amounts of ferric iron can exist in solution), which offers an inorganic hypothesis limiting ferric iron availability for precipitate formation in H₂-containing *M. sedula* cultures (where dissolved oxygen concentrations available for precipitate formation are also reduced). An organic hypothesis suggests the possibility of biological coupling of H₂

oxidation to ferric iron reduction (concomitant with the predominating biological oxidation effect observed in Fig 1B), that would limit ferric iron availability for precipitate formation.

Specific bioleaching rates are negatively impacted by the presence of H₂. To determine the impact of H₂ on specific bioleaching rates, cell density and total soluble iron were tracked for 6 days following inoculation for *M. sedula* cultures with an air headspace enhanced with H₂+CO₂ or CO₂. Following harvest of CO₂-enhanced cultures (no H₂ present), which had iron precipitate on vessel walls that was similar to air-only headspace cultures (no H₂ or CO₂ present, data not shown), the precipitate adhering to the wall was dissolved using 10 N HCl; the working volumes were then restored to that of the initial culture. The resulting total soluble iron levels were determined, such that the total iron release reported for CO₂-enhanced cultures includes contributions from the precipitate that accumulated on culture vessel walls. It should be noted that 6 days after inoculation, total iron levels in solution were the same for air headspace cultures as for CO₂-enhanced headspace cultures (data not shown); no iron contribution from wall precipitates was included for air-only cultures. Specific bioleaching rates were calculated by dividing the average cell density (note cells were counted in a 2 dimensional space, therefore cells attached to the bottom of particles would have been missed for both culture conditions) during the 6-day post-inoculation period by the total amount of iron released from the chalcopyrite during the same time. The specific leaching rate for H₂+CO₂-enhanced cultures was 5.1×10^{-10} mg Fe/cell compared to 2.8×10^{-9} mg Fe/cell for CO₂-enhanced cultures, or greater for the CO₂-enhanced cultures. There was no significant difference in total iron released biotically from H₂+CO₂- or CO₂-enhanced cultures during this period (55 mg/L vs. 62 mg/L, respectively). However, the difference in average planktonic cell densities (1.1×10^8 cells/mL of H₂-containing culture compared to 2.2×10^7 cell/mL of CO₂-enhanced culture) indicated that H₂-supplemented cultures were less efficient in

bioleaching (total iron release) on a per cell basis. The higher biomass and faster growth rates in the H₂ + CO₂-enhanced cultures compared to the “air-only” or CO₂-enhanced cultures indicated that H₂ was serving as an alternate energy source for *M. sedula*.

Competition between H₂ and Fe²⁺ as energy sources. Components of electron transport chains in *M. sedula* have been examined with respect to iron and sulfur oxidation activities, as this relates to bioleaching capabilities (2, 3). **Figure 2** shows these components and their transcriptional response when exposed to chalcopyrite for up to 9 days, and **Table 1** provides detailed transcriptomic information.

Components of electron transport chains associated with Fe²⁺-based electron sources were activated upon exposure to chalcopyrite, indicating that Fe²⁺ was being utilized as an energy source. These components included *soxNL* and *cbsA'A* (cytochrome b), the *foxA* transcript from the *fox* cluster originally described in the iron oxidizer *Sulfolobus metallicus* (5), a putative rusticyanin (Msed_0966), a terminal oxidase (*doxBCE*, Msed_2032, 2031, 2030) previously described in *Acidianus ambivalens* (18), and a putative pyruvate:ferredoxin oxidoreductase (Pfor $\gamma\delta\alpha\beta$, Msed_0507-0510). Consistent with previous observations for growth on soluble iron (2, 3), the *soxNL-cbsA'A* transcripts were all significantly up-regulated in the presence of chalcopyrite (d9) compared to the inoculum (d0). While the *foxA'BCD* (Msed_0485, 0480, 0478, 0477) transcripts were down-regulated in the presence of chalcopyrite (d9 vs. d0), the *foxA* (Msed_0484) transcript was up-regulated after exposure to chalcopyrite (d3 vs d0). This suggests that the utility of FoxAA'BCD for electron transport from Fe²⁺ correlates with activation of the *foxA* and down-regulation of *foxA'* transcripts. Of particular note is the 10.5-fold (p-value 2.3 x 10⁻⁶) up-regulation of *rus* (Msed_0966, d9 vs d0); the encoded putative protein in this ORF, a rusticyanin homolog, has been implicated in electron transfer from Fe²⁺ in the model mesophilic bioleaching organism, *Acidithiobacillus ferrooxidans* (20). Here, maximum

soluble iron levels were < 0.2 g/L, significantly lower than the soluble iron levels from previous *M. sedula* studies (2.7 – 3.7 g-Fe/L) in which no significant differential transcription of *rus* was reported. Thus, transcription of this *M. sedula* gene may be triggered by additional factors beyond soluble iron levels.

Downstream of *pfor*, the gene encoding a putative pyruvate synthase converting acetyl-CoA from inorganic carbon fixation into pyruvate using electrons from reduced ferredoxin (Auernik and Kelly, unpublished data), are several hypothetical proteins (Msed_0511, 0512, 0515) that are homologs (24-32% identity) to bacterial PqqE proteins implicated in pyrrolo-quinoline quinone cofactor biosynthesis (9, 10, 14), and a hypothetical protein (Msed_0518) similar to several uncharacterized flavoproteins. As was previously noted on soluble iron, these ORFs were up-regulated on chalcopyrite (**Table 1**).

Hydrogenase accessory and maturation transcripts did not respond differentially to the growth conditions studied here, although both the α subunit (Msed_0945) and the membrane anchor (Msed_0946) of the primary hydrogenase were down-regulated from day 3 to day 9. Despite this response, transcripts for the hydrogenase genes were still highly transcribed at day 9. This indicates that while H₂ was no longer the primary energy source, *M. sedula* was still deriving bioenergetic benefit from molecular hydrogen. The heterodisulfide-like cluster (Msed_1542-1549), which is likely involved in electron transfer from hydrogenases (Auernik and Kelly, unpublished results) and reduced inorganic sulfur compounds (RISCs) (2), was highly transcribed here; unlike the hydrogenase structural components, it did not change from day 3 to 9. Transcripts for the *soxABCDD'* terminal oxidase, activated when exposed to either RISCs or H₂, were differentially transcribed when exposed to chalcopyrite. The ORF encoding *soxDD'* (Msed_0285/Msed_0286) was up-regulated upon exposure to chalcopyrite and transcripts for the Rieske protein, encoded by *soxL* (Msed_0288), was down-regulated from day 3 to day 9. A putative sulfide:quinone reductase (Msed_1039, *sqr*-like), predicted to be targeted to the outside of the membrane

by both SignalP and the archaeal PRED-SIGNAL (3, 4), was up-regulated 3.4-fold (p-value 6.3×10^{-10}) from day 3 to 9. The down-regulation of several hydrogenase components, combined with the up-regulation of several ORFs possibly involved in sulfur oxidation and lack of response from the *hdr*-like cluster thought to utilize both energy sources, suggests that RISCs may also be serving as an inorganic energy source by day 9.

Although it is clear that the inoculum used for chalcopyrite cultures was growing autotrophically on inorganic carbon and H_2 , it is unclear what growth mode(s) characterize growth on chalcopyrite. Multiple inorganic energy sources are available - chalcopyrite provided a source of Fe^{2+} and RISCs, in addition to the H_2 present in the headspace. Once in stationary phase, a potential source of organic carbon (and possibly an energy source) are proteins and peptides released through cell lysis. Several transcripts encoding enzymes of the 3-hydroxypropionate/4-hydroxybutyrate cycle of inorganic carbon fixation were highly transcribed at day 0 and day 3, but decreased by day 9: the putative carbonic anhydrase (Msed_0390), the acetyl-/propionyl-CoA carboxylase (Msed_0147, 0148, 1375), and malonyl-/succinyl-CoA reductase (Msed_0709). This suggested that *M. sedula* was switching away from inorganic carbon fixation, most likely in favor of an organic carbon source, a strong preference based on previous mixotrophy studies (Auernik and Kelly, unpublished results). This is further supported by up-regulation of several transcripts associated with TCA intermediate cycling (Msed_1581/Msed_1582), aromatic amino acid catabolism (Msed_1772-Msed_1777), and removal of excess N from organic carbon substrates (Msed_2074) (data not shown). It is not clear if this organic carbon also serves as a competitive energy source, but it has the potential to negatively impact inorganic energy utilization by reducing inorganic carbon fixation.

While supplementing *M. sedula* bioleaching cultures with H_2 offers a method to build biomass and reduce potentially undesirable ferric iron compound precipitation, it also reduces specific bioleaching rates (both directly and indirectly). Further studies are needed

to understand the energy metabolism of *M. sedula* (and related extreme thermoacidophiles) in order to optimize their function as bioleaching agents (1).

ACKNOWLEDGEMENTS

We would like to thank Greg Olsen for providing the chalcopyrite used in this work. KSA acknowledges support from the NCSU Molecular Biotechnology Training Program through an NIH T32 Biotechnology Traineeship. RMK acknowledges support from the NSF Biotechnology Program and from the U.S. Defense Threat Reduction Agency (DTRA).

REFERENCES

1. **Auernik, K. S., C. R. Cooper, and R. M. Kelly.** 2008. Life in hot acid: pathway analyses in extremely thermoacidophilic archaea. *Curr Opin Biotechnol* **19**:445-53.
2. **Auernik, K. S., and R. M. Kelly.** 2008. Identification of components of electron transport chains in the extremely thermoacidophilic crenarchaeon *Metallosphaera sedula* through iron and sulfur compound oxidation transcriptomes. *Appl Environ Microbiol* **74**:7723-32.
3. **Auernik, K. S., Y. Maezato, P. H. Blum, and R. M. Kelly.** 2008. The genome sequence of the metal-mobilizing, extremely thermoacidophilic archaeon *Metallosphaera sedula* provides insights into bioleaching-associated metabolism. *Appl Environ Microbiol* **74**:682-92.
4. **Bagos, P. G., K. D. Tsirigos, S. K. Plessas, T. D. Liakopoulos, and S. J. Hamodrakas.** 2009. Prediction of signal peptides in archaea. *Protein Eng Des Sel* **22**:27-35.
5. **Bathe, S., and P. R. Norris.** 2007. Ferrous iron- and sulfur-induced genes in *Sulfolobus metallicus*. *Appl Environ Microbiol* **73**:2491-7.

6. **Breitkreutz, B. J., P. Jorgensen, A. Breitkreutz, and M. Tyers.** 2001. AFM 4.0: a toolbox for DNA microarray analysis. *Genome Biol* **2**:SOFTWARE0001.
7. **Clark, T. R., F. Baldi, and G. J. Olson.** 1993. Coal Depyritization by the Thermophilic Archaeon *Metallosphaera sedula*. *Appl Environ Microbiol* **59**:2375-2379.
8. **Du Plessis, C. A., J. D. Batty, and D. W. Dew.** 2007. Commercial Applications of Thermophile Bioleaching. In D. E. Rawlings and D. B. Johnson (ed.), *Biomining*. Springer-Verlag, Berlin Heidelberg.
9. **Felder, M., A. Gupta, V. Verma, A. Kumar, G. N. Qazi, and J. Cullum.** 2000. The pyrroloquinoline quinone synthesis genes of *Gluconobacter oxydans*. *FEMS Microbiol Lett* **193**:231-6.
10. **Goosen, N., H. P. Horsman, R. G. Huinen, A. de Groot, and P. van de Putte.** 1989. Genes involved in the biosynthesis of PQQ from *Acinetobacter calcoaceticus*. *Antonie Van Leeuwenhoek* **56**:85-91.
11. **Han, C. J., and R. M. Kelly.** 1998. Biooxidation capacity of the extremely thermoacidophilic archaeon *Metallosphaera sedula* under bioenergetic challenge. *Biotechnol Bioeng* **58**:617-24.
12. **Harvey, T. V. D. M., W.** 2002. Presented at the Bio & Hydrometallurgy, Capetown, South Africa.
13. **Kappler, U., L. I. Sly, and A. G. McEwan.** 2005. Respiratory gene clusters of *Metallosphaera sedula* - differential expression and transcriptional organization. *Microbiology* **151**:35-43.
14. **Meulenberg, J. J., E. Sellink, N. H. Riegman, and P. W. Postma.** 1992. Nucleotide sequence and structure of the *Klebsiella pneumoniae* pqq operon. *Mol Gen Genet* **232**:284-94.

15. **Muir, M. A., T.** 1977. Determination of Ferrous Iron in Copper-Process Metallurgical Solutions by the o-Phenanthroline Colorimetric Method Metallurgical transactions. B, Process metallurgy **8B**:517-518.
16. **Norris, P. R., N. P. Burton, and N. A. Foulis.** 2000. Acidophiles in bioreactor mineral processing. Extremophiles **4**:71-6.
17. **Olson, G. J., J. A. Brierley, and C. L. Brierley.** 2003. Bioleaching review part B: progress in bioleaching: applications of microbial processes by the minerals industries. Appl Microbiol Biotechnol **63**:249-57.
18. **Purschke, W. G., C. L. Schmidt, A. Petersen, and G. Schafer.** 1997. The terminal quinol oxidase of the hyperthermophilic archaeon *Acidianus ambivalens* exhibits a novel subunit structure and gene organization. J Bacteriol **179**:1344-53.
19. **Valdes, J., I. Pedroso, R. Quatrini, R. J. Dodson, H. Tettelin, R. Blake, 2nd, J. A. Eisen, and D. S. Holmes.** 2008. *Acidithiobacillus ferrooxidans* metabolism: from genome sequence to industrial applications. BMC Genomics **9**:597.
20. **Yarzabal, A., C. Appia-Ayme, J. Ratouchniak, and V. Bonnefoy.** 2004. Regulation of the expression of the *Acidithiobacillus ferrooxidans* *rus* operon encoding two cytochromes c, a cytochrome oxidase and rusticyanin. Microbiology **150**:2113-23.

TABLE 1: Transcriptional response for inorganic energy source utilization.				
Category / Function	ORF	Annotation	Change (n-fold)	Time point comparison (days)
Iron oxidation	Msed_0467	transporter	+6.8	0 vs 9
	Msed_0469	<i>foxG</i>	+3.8	0 vs 9
	Msed_0477	<i>foxD</i>	+6.3	0 vs 9
	Msed_0478	<i>foxC</i>	+5.8	0 vs 9
	Msed_0479	unique hypothetical protein (80aa)	+15.1	0 vs 9
	Msed_0480	<i>foxB</i>	+12.5	0 vs 9
	Msed_0484	<i>foxA</i>	-3.0	0 vs 3
	Msed_0485	<i>foxA'</i>	+5.1	0 vs 9
	Msed_0486	CBS domain	-11.5	0 vs 9
	Msed_0500	<i>soxN</i>	-3.0	0 vs 9
	Msed_0501	<i>soxL2</i>	-4.7	0 vs 3
	Msed_0502	<i>cbsA'</i>	-3.6	0 vs 9
	Msed_0504	<i>cbsA</i>	-3.2	0 vs 9
Fe / inorganic electron transport	Msed_0966	<i>rus</i>	-10.5	0 vs 9
	Msed_0510	<i>pfor</i> β	-3.7	0 vs 3
	Msed_0511	<i>pqqE</i> -like	-15.5	0 vs 3
	Msed_0512	<i>pqqE</i> -like	-24.3	0 vs 3
	Msed_0513	conserved hypothetical	-20.0	0 vs 3
	Msed_0514	U32 peptidase	-18.7	0 vs 3
	Msed_0515	<i>pqqE</i> -like	-6.0	0 vs 3
Fe oxidation / S oxidation	Msed_0516	conserved hypothetical	-6.4	0 vs 3
	Msed_2030	<i>doxE</i>	-11.4	0 vs 9
	Msed_2031	<i>doxC</i>	-2.4	0 vs 9
	Msed_2032	<i>doxB</i>	-5.1	0 vs 9
	Msed_0570	<i>doxB2</i>	-3.7	0 vs 9
	Msed_1039	<i>sqr</i> -like	-3.4	0 vs 9
S oxidation / H ₂ utilization	Msed_0364	<i>doxA</i>	-3.1	0 vs 9
	Msed_0285	<i>soxD</i>	-2.5	0 vs 3
	Msed_0286	<i>soxD'</i>	-3.0	0 vs 3
	Msed_0288	<i>soxL</i>	+2.4	3 vs 9
H ₂ -utilization	Msed_0945	<i>hynL</i>	+4.7	3 vs 9
	Msed_0946	<i>isp1</i>	+3.6	3 vs 9
	Msed_0948	conserved hypothetical	+4.4	3 vs 9
	Msed_0949	conserved hypothetical	+3.9	3 vs 9
Inorganic carbon fixation	Msed_0390	carbonic anhydrase	+3.4	3 vs 9
	Msed_0147	acetyl-/propionyl-CoA carboxylase	+5.6	3 vs 9
	Msed_0148	acetyl-/propionyl-CoA carboxylase	+3.3	3 vs 9
	Msed_1375	acetyl-/propionyl-CoA carboxylase	+4.7	3 vs 9
	Msed_0709	malonyl-/succinyl-CoA reductase	+5.7	3 vs 9

FIGURES

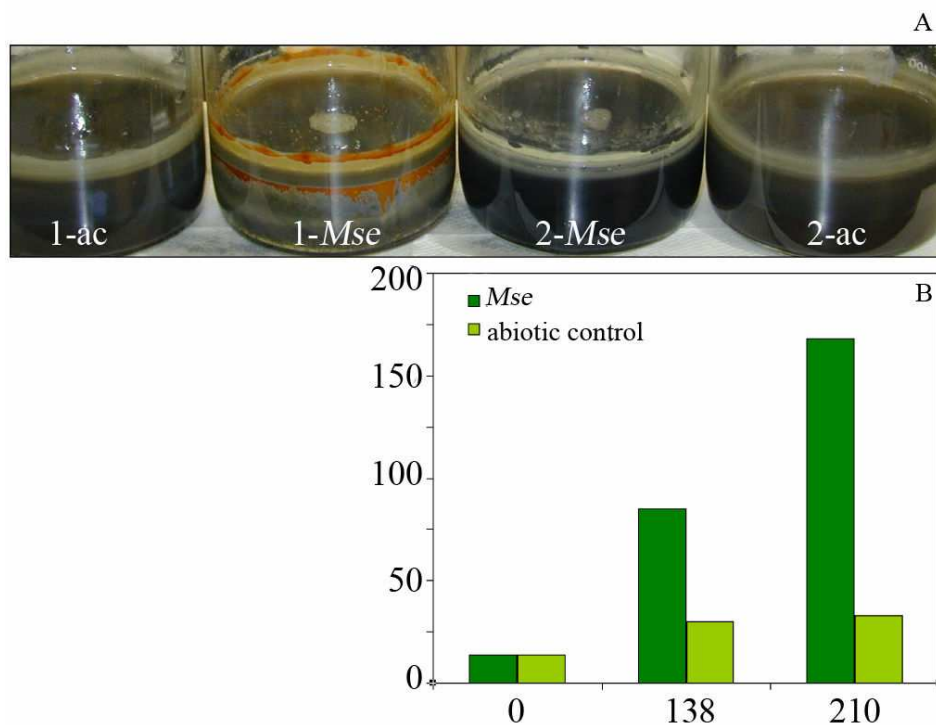


Figure 1: Chalcopyrite bioleaching by *M. sedula*.

A) Nine days post-inoculation, chalcopyrite bioleaching by *M. sedula* exposed to an air headspace (1-*Mse*) is visually evident compared to its abiotic control (1-ac). No obvious evidence of bioleaching is visible for *M. sedula* grown in a hydrogen-containing headspace (2-*Mse*) or the associated abiotic control (2-ac).

B) Measurement of the total soluble iron (mg/L) as a function of hours post-inoculation shows that cultures containing *M. sedula* grown in a hydrogen-containing headspace are significantly higher than the abiotic control, indicating active bioleaching. Typical standard deviations of < 10 mg/L were found for the iron assay (n=3 for abiotic controls; n=9 for *M. sedula* cultures)

